8-6-2021

An analysis of human gait under slippery conditions using OpenSim's musculoskeletal simulations

Phong K. Phan
pkphong0606@gmail.com

An analysis of human gait under slippery conditions

using OpenSim's musculoskeletal simulations

By

Phong K. Phan

Approved by:

Steven H. Elder (Major Professor/Graduate Coordinator)
Raj K. Prabhu
Reuben F. Burch
Harish Chander
David Macias
Jason M. Keith (Dean, Bagley College of Engineering)

A Thesis
Submitted to the Faculty of
Mississippi State University
in Partial Fulfillment of the Requirements
for the Degree of Master of Science
in Biomedical Engineering
in the Department of Agricultural and Biological Engineering

Mississippi State, Mississippi

August 2021

Name: Phong K. Phan

Date of Degree: August 6, 2021

Institution: Mississippi State University

Major Field: Biomedical Engineering

Major Professor: Steven H. Elder

Title of Study: An analysis of human gait under slippery conditions using OpenSim's musculoskeletal simulations

Pages in Study: 46

Candidate for Degree of Master of Science

Computational simulations of gait under abnormal conditions provide insights into the actions of muscles, its relationships with external reaction forces and motions of the body during slips, trips, and falls—the leading causes of occupational injuries worldwide. OpenSim™, an open-source motion simulation software, was utilized to construct musculoskeletal structures and create dynamic simulations of body movements. Gaits of eighteen subjects were studied to extract experimentally difficult-to-obtained variables under slippery conditions. The joint angles and moments of hip, knee, ankle and the forces of four prime muscle groups were analyzed for body corrective movements during slip events. Besides, the connections between one's perception of the surrounding environment and their postural alterations to prevent falls are also discussed. Hence, this study provides a better understanding on the joint angles, moments and muscle forces of human body, evaluates the movement deviations, and contributes to the development of predictive injury thresholds during slip events.

ACKNOWLEDGEMENTS

I would like to express my gratitude to my advisors, Dr. Raj Prabhu, Dr. Reuben Burch and Dr. Harish Chander for always encouraging and believing in me. I am truly grateful for their constructive guidance and support, as well as for their insightful knowledge and experience in simulation, modeling and human biomechanics aspects. Without these instructions, it would not be possible for me to accomplish this project. I'm also thankful to Dr. Steven Elder and Dr. David Macias for their kindness and assistance during the time I prepared this thesis. Despite the short time we had, they have helped me review my work and supporting me in every possible way.

Furthermore, I would like to thank my friends and family for their assistance and positive spirit, especially Ms. Anh Vo, who always gave me helpful advices, and went through ups and downs with me during the time conducting this study.

Finally, this work was supported by the Center for Advanced Vehicular Systems (CAVS) and the Department of Agricultural and Biological Engineering (ABE) at Mississippi State University. Also, thanks to the support from CAVS and ABE faculties and staffs, I am able to conduct and complete this research with the all the best conditions I could have."

TABLE OF CONTENTS

LIST OF TABLES

LIST OF FIGURES

CHAPTER I

INTRODUCTION

1.1 Motivation

Occupational slips, trips, and falls (STFs) are a leading cause of substantial injuries worldwide, especially in slip-prone environments such as hospitals and clinics, posing a great burden to the health of workers as well as to the financial loss of the companies. According to the US Bureau of Labor Statistics, in the year of 2018, there are a total of 126,850 cases of non-fatal workplace injuries as well as 791 (15%) out of 5,250 cases of workplace fatalities due to STFs [1]. Specifically, STFs are the results of a failure of normal locomotion together with a failure of attempts at equilibrium recovery following an induced gait imbalance [2,3]. There are two main factors that induce STFs: environmental factors (extrinsic) and human factors (intrinsic). For example, the extrinsic factor involves the physical characteristics of the floor surface, such as the type, the smoothness, or roughness of the surface as well as the presence of contaminant or the interaction of the footwear with the floor [3,4]. In contrast, the intrinsic factor strongly connects with the human element, which can be a result of aging, anthropometric features, gait speed, muscle fatigue, slipperiness perception, and even disorders of the musculoskeletal system [3–5]. The slip propensity is generated and escalated when friction between feet and walking surfaces are not large enough to prevent the hindfoot from sliding as it pushes off, or the forefoot from sliding when it tries to slow the forward motion of the human body's center of gravity during normal gait [4,6,7]. Different terminologies are used to classify

various STFs cases in term of the slip distances, recovery, and perception of the slipping. Particularly, Perkins et al. groups slips into macro-slips and micro-slips depending on the slip distance from heel motion to distinguish the slip severity [8]. Strandberg et al., conversely, differentiate slips into three categories with respect to the three levels of slip perception and recovery: (a) mini-slips (no slipping motion detected), (b) midi-slips (slipping detected and recover with minor gait disturbances), and (c) maxi-slips (slipping recovery involving large corrective response) [9]. McGorry et al. identified that most hazardous slips happen during the time period of 25 ms immediately after heel strike, which plays an important role in the development of an unrecoverable slip propensity [7]. Lockhart et al. also made similar conclusions that the time period of < 70-120 ms after the first heel strike has great impact on the slip propensity development [10]. Hence, the time period of 120 ms post heel strike is crucial in analyzing the slip initiation as well as predicting the potential outcome of the impending slips.

Subjective perception of the floor slipperiness based on visual perception and proprioceptive recognition of balance maintenance also plays a major role in a development of slip events [11]. For example, all external factors such as floor color, shape, size, texture, lightning, and internal factor such as visual perception, attentiveness and mental clarity can affect the outcome of perceiving the slippery surface [12][13]. Due to these factors, the body can modify its gait pattern to reduce the possibility of slip events. These modifications might include postural changes, and adaptation during gait cycle, decreased step length, low-impact ground reaction forces, and altered joint moments [14]. Additionally, in the event of alerted or expected slips, muscle activities of the lower extremity appear to be greater and faster. To be more precise, the pairs of prime mover muscles in the ankle (tibialis anterior and medial gastrocnemius) and at the knee (vastus lateralis and medial hamstrings) were reported to have great activities and

muscle co-contraction leading to a stable gait and prevented the slip events from happened [15]. As a result, analyzing these prime mover muscles can also be a potential approach in determining human biomechanics during a slip event.

1.2 Slips-trips previous studies

In general, the biomechanical analysis of slips aids in the evaluation of the description of motion of the body-segments as well as the interaction of the footwear-floor interface during a slip event [13,16]. Joint angles have been one of the most investigated properties in analyzing the characteristics of STFs during both normal and dry conditions [17,18] as well as under slippery conditions [19–21]. Particularly, during a normal gait on a dry surface, the ankle is in either neutral or slight dorsiflexion position at heel strike, which is followed by a quick roll into plantarflexion position as the foot moves to mid-stance phase. During the same period, the leg is raised and moved forward while the hip joints decline from its maximum flexion angle at heel strike to extension positions throughout the gait cycle [18]. However, this pattern changes when the gait is performed on a slippery surface. To be more precise, comparing to the dry condition, the gait under slippery condition yields an increase in plantarflexion of ankle joint [20], a greater foot-floor angle, and a greater hip flexion angle at heel strike [4], all of which contribute to a greater incidence of slips. During the slip, Redfern et al. found that the hip flexion angle was minimized while the knee flexion was increased, which could be considered as a corrective movement of the human body in an attempt to adjust the center of mass within the base of support and prevent potential falls [4]. Various studies have been performed, aiming to investigate and analyze such a corrective movement of the body. For example, electromyographic (EMG) recordings can indicate when a muscle is active during a gait cycle and is often used to study the relationship between muscle activities and gait kinematics, muscle

pains or disability and rehabilitation [22,23]. However, an examination of EMG recordings did not allow researchers to accurately identify which motion of the body was caused by a particular muscle activity [24]. Determining how individual muscles contribute to a specific motion is challenging as a muscle can accelerate joints that it does not span and affect the body segments that it does not directly attach to [24].

Hence, creating an integrated understanding of normal gait pattern as well as establishing a scientific basis for correcting abnormal movement has always been a major challenge until the application of computational simulations during recent years. Particularly, dynamic simulations of movement enable one to intensively study neuromuscular coordination, analyze athletic performance, and evaluate the internal loading distributions in the musculoskeletal system [25]. Muscle-driven dynamic simulations complement experiments as they can provide estimates of generally improbable-to-measure variables (such as muscle forces and joint moments) that offer insights into both muscle function and human movement control [17]. Moreover, computational models and simulations developed using experimental data are usually used to generate the muscle-tendon dynamics, musculoskeletal geometry, and multibody dynamics transformations of a simulated neural control in a specific movement [17]. For example, simulation can be used to identify the sources of pathological movement and determine a scientific basis for treatment planning [24]. Additionally, one of the more empowering features of simulations is the potential to perform 'what if' studies to test various hypotheses, predict a functional outcome, and detect irregular behaviors [17].

1.3 Overview and Application of OpenSim™

Among all the biomechanical modeling software currently used by hundreds of biomechanics laboratories around the world, OpenSim™ is one of the most widely used open-

source platforms. OpenSim™ enables users to develop musculoskeletal structure models and create dynamic simulations of movement in a broad range of scenarios, which include analysis of walking dynamics, studies of sports performance, simulations of surgical procedures, and analysis of joint loads and design of medical devices [26–31]. The graphical user interface of OpenSim™, developed and maintained on Simtk.org—a public repository for physics-based data, models, and computational tools—includes a suite of tools for analyzing musculoskeletal models, generating simulations, and visualizing results [24]. OpenSim™ also supports a large and growing community of biomechanics and rehabilitation researchers and creates a platform on which the biomechanics community can build tools, exchange models and simulation for reproducing and extending discoveries. This type of platform can help uncover the human movement mechanism and assist in the design of a better treatment procedures for individuals with disabilities [32]. OpenSim™ unites the interaction of complex neural muscular and skeletal systems to create a fast and accurate simulation of movements. One of OpenSim™ applications is the ability to compute variables that are difficult to measure experimentally, such as the force generated by the muscle or the tendons' fiber length during specific movement [25]. Another application of OpenSim™ is to predict novel movements from models of motor control (also known as actuator control) such as kinematic adaptations of human gait during different walking conditions (inclined, declined, tilted, dry or slippery surface, etc.) [32]. Additionally, OpenSim™ can be used to simulate and evaluate the change in the musculoskeletal system following surgery or due to human-device interactions such as implants and prostheses—which plays an important role in the design of implantable medical prosthesis devices to improve the quality of life of patients with paralysis [32]. Likewise, simulations in OpenSim™ are generally validated by how closely they agree with the experimentally measured kinematics, kinetics, and EMG patterns of

the interested movement, all of which demonstrate the complement between simulations and experiments. Finally, once a simulation is generated and accurately tested, it can be further analyzed to identify the contributions of a muscle on a particular motion of the body as well as its potential outcomes [17].

1.4 Objective

Even though there are various studies that utilize OpenSim™ to analyze gait cycle in different environments [26,28,33,34], none of them have investigated OpenSim™'s ability to evaluate gait under slippery conditions. More specifically, using gait data from a motion capture system, OpenSim™ can extract assorted variables that otherwise wouldn't be obtained from experiments alone. Using OpenSim™ in analyzing slip-trip data taken from previous studies proposes a new approach in examining gait cycles with the potential of extracting the more insightful information while using the minimum amount of input variables and laboratory equipment. For example, in Chander et al.'s works, marker trajectory data of normal gait and gait under slippery conditions with different footwears as well as slip perceptions were obtained from experiments using a motion capture system, force plates, and EMG sensors [35,36]. However, variables such as muscle activations, muscle forces, joint angles, and moments at various locations on the human body could not be achieved due to the limitation in the number of markers attached to the participants as well as the limited EMG channels (sensors) used in a particular time. Hence, if these slip and trip gait data are processed in OpenSim™ to develop a corresponding simulation, then (a) the aforementioned immeasurable variables can be obtained, (b) the number of equipment used in the experiment can be reduced, and (c) the total number of extracted information from a given experiment can be maintained or even increased. Therefore, the objective of this study is to determine if simulations in OpenSim™ using slip-trip data (from

the Chander et al. study [35]) is a practical alternative method of examining gait data and can provide a deeper understanding of the effect of slip perception under multiple gait conditions. This can be done by firstly extracting and converting motion capture gait data into OpenSim™ formats. Then, various simulation optimizations would be performed on the musculoskeletal system in OpenSim™ to attain some pre-determined joints and muscles' joint angles and fiber forces. Specifically, three joints (hip, knee, and ankle) and four groups of prime muscles (bicep femoris – BF, medial gastrocnemius – MG, tibialis anterior – TA, and vastus intermedius – VI) [37] are selected based on the group of joints and muscles analyzed in Chander et al.'s experimental studies [11,35]. Due to the limitation of available groups of muscle on the musculoskeletal model, the vastus intermedius muscle is chosen instead of the vastus lateralis muscle used in Chander et al.'s studies [11,35]. Finally, the simulated data is post-processed and plotted in MATLAB™ (The Mathworks Inc., Natick, MA) and the conclusions area drawn based on these results.

CHAPTER II

METHODS AND SIMULATION SETUP

2.1 Data Acquisition

The analyzed slip-trip data used in this work was achieved from Chander et al. slip-trip gait analysis [11,35]. Specifically, eighteen healthy male participants (age: 22.28 ± 2.2 years; height: 177.66 ± 6.9 cm; mass: 79.27 ± 7.6 kg) were recruited for the data acquisition procedure [35]. These volunteers were ensured to have no history of musculoskeletal injuries, cardio-vascular abnormalities, neurological or vestibular disorders. All recruited participants were approved by the University's Institutional Review Board (IRB) and their informed consent and a physical activity questionnaire (PAR-Q) were also collected. In the Chander et al. study, the experimental set up included a Vicon Nexus™ (Vicon Motion Systems Ltd, UK) 3D motion capture system with 12 infra-red T-series cameras, two force plates (Bertec™ [Bertec Corporation, USA] and AMTI™ [AMTI Force and Motion, USA]) and a Noraxon Telemyo™ DTS 900 EMG system (Noraxon, USA) was used to collect and analyze kinematic, kinetic and muscle activity data during gait. A slippery agent, which is a mixture of industrial vegetable-based glycerol and water with the ratio of 3:1, was applied on the force plate to lubricate the participant walking surface [35]. Chander et al. used a uni-track fall arrest system from Rigid Lines™ (Millington, TN) to prevent participants from any undesired falls [35]. Four types of gait conditions conducted in the study of Chander et al. were assessed including (a) normal gait (NG), (b) unexpected slip (ES), (c) alerted slip (AS), and (d) expected slip (US) [35]. The NG

trial was comprised of a repeated number of gait cycle under normal dry condition. Whereas, the US, AS, and ES trials were conducted under different instructions given to the participants. In the case of US trial, the participants would perform a gait cycle without the expectation of slippery agent applying on the force plate, making them prone to slip. Then, they repeated the experiment again with an instruction that the floor 'may be slippery' for AS trial. Lastly, the participant would perform the last ES trial with the knowledge of the slippery floor. Hence, the three trials US, AS, and ES characterize an increasing scale of participants' perception of the slippery surface.

In the previous works of Chander et al. [11,35], the participants walked on the lubricated surface wearing one of the three footwears (Crocs™, flip-flops, and low top slip resistant shoes). However, in this study, only the gait data of the low top slip resistant shoes were extracted, converted, and analyzed in OpenSim™ as it is the most stable case among the three, which can reduce errors in the conversion process. After selecting the correct gait data from motion capture, a series of in-house developed codes were utilized to extract, convert, and analyze the gait cycle in MATLAB™ R2016a (The Mathworks Inc., Natick, MA). Specifically, there are two types of input files for OpenSim™: the traction file (.TRC), which contains the experimental marker trajectories, and the motion file (.MOT), including the set of external load data such as ground reaction forces, moments, and center of pressure locations. Another important property when converting data from motion capture into OpenSim™ is the coordinate axes. For example, in the motion capture system, X and Y axes represents the ground while Z axis is the vertical direction; however, X and Z axes span the ground in OpenSim™ and the Y axis represents upward. Hence, the coordinate of the markers and forces need to be swapped accordingly from [X Y Z] system to [X -Z Y] system.

After being extracted and converted, the gait data must be cropped and aligned correctly based on a particular time window. According to McGorry et al., the period of 25 ms starting from the first heel strike plays an important role in the initiation of an unrecoverable slip propensity [7]. Hence, to focus on the slip development post heel strike, the time frame between the moment of the first heel strike phase until the following toe-off phase on the slippery force plate is chosen to crop the gait data. In Chander et al. works [11,35], whose data consist of approximately three gait cycles per trial, this particular time window is considered as the middle left heel-strike phase to the middle left toe-off phase. The specific frames of these two boundaries were also identified and collected using the motion capture system. Therefore, using this information, the converted gait data were cropped properly with respect to the acquired time window. Finally, the gait data were scaled base on the percentage task duration of the time window. This was done using interpolation with spline method in MATLAB™ R2016a (The Mathworks Inc., Natick, MA), in which the gait data were rescaled into 101 points. The x-axis values of these points were corresponding to the time stamps of 0% to 100% in the specific time window of a distinct trial. The task duration was further divided into three phases: Phase 1 (0%-20% duration), Phase 2 (21%-83% duration) and Phase 3 (84%-100% duration). According to Stockel et al., these phases fully captured the stance phase of the left foot on the slippery force plate, which consists of initial contact – weight acceptance phase (Phase 1), single support phase (Phase 2) and pre-swing phase (Phase 3) [38]. Then, the average data between all participants for each trial at each phase were computed and recorded. The standard deviation between the participants were calculated and plotted together with the average values.

For the purpose of this study, the data of three common joint angles and moments (hip, knee, and ankle in sagittal plane, representing flexion movements) as well as the fiber force of

four prime movers [37] – BF, MG, TA, and VI – were extracted and analyzed. These data came from the subjects' left foot in the pre-specified time window during four gait trials (NG, US, AS, and ES). Then, the NG cases were used as the reference when comparing with the other cases to identify the influence of slippery perception on the human's corrective movements to prevent falls.

2.2 OpenSim™ Model

For this study, the 'gait2392' human musculoskeletal model, developed by Delp et al. [24], were used to analyze the slip-trip gait data. Included with the OpenSim™ Distribution, the 'gait2392' model featured 23-degree-of-freedom with 92 musculotendon actuators in the lower extremities and torso of the human musculoskeletal system [39]. Unlike its counterpart—model 'gait2354', the 'gait2392' model is a complex version with more muscles, aiming to improve simulation accuracy for demonstrations and educational purposes [39]. Specifically, this version was configured to have three degrees of freedom at the hip (flexion, adduction, and rotation), one degree of freedom at the knee (flexion), and two degrees of freedom at the ankle (flexion and rotation). Meaning that, for this particular model, OpenSim™ was focused on analyzing the gait cycle of the hip, knee, and ankle with respect to the flexion plane (i.e., sagittal plane or anterior-posterior direction).

Besides, this model consists of three main components: bone, muscle and actuator. Bones can be imported from computer-aided design (CAD) files of individual bone, which can also be replaced by prosthesis designs if needed. Muscles (shown as red tube on the model) are created using a number of muscle points, which indicate the route of a muscle along the body and are connected together by the muscle paths. To accurately simulate the muscles' behaviors due to the body movements, there are various options in OpenSim™ to adjust and modify the muscle

points and paths so that they can wrap around a bone when a specific joint angle is reached. Muscles are mathematically represented as a parallel spring and damper system in OpenSim™. The last component is the actuator, which is an invisible component that attached at each joint and muscle to apply the corresponding moments and forces when needed. Besides the muscle actuator, which is the muscle itself, there are two other type of actuators, reserve and residual. Reserve actuators are on the joints and are used to drive the model when no muscles are present or when muscles are not sufficient to track input kinematics. Residual actuators are located on the base segment (pelvis in this case) to supply additional forces that accounted for the errors in the model. Especially, residual actuators are recruited when the kinematic that do not balance with experimental ground reaction forces. The residual forces created by the residual actuator compensate for the dynamic inconsistencies between kinematic and kinetic data.

Additionally, based on the studies of Chander et al. [11,35], 16 virtual markers were placed on the model according to the Helen-Hayes marker system, which is one of the most common marker arrangements utilized in 3D motion analysis [40]. Notably, the Helen-Hayes marker system had been applied efficiently in routine clinical practice to study the mechanics of the gait patterns of many patients with various conditions [41]. In this case, each of the limbs contained eight virtual markers, located from the pelvis down to the toes. This specific arrangement of marker locations was identical to the markers placed on the subjects during the experimental trial in Chander et al. studies [11,35]. The illustration of the marker locations on the musculoskeletal model is shown in Figure 2.1 below.

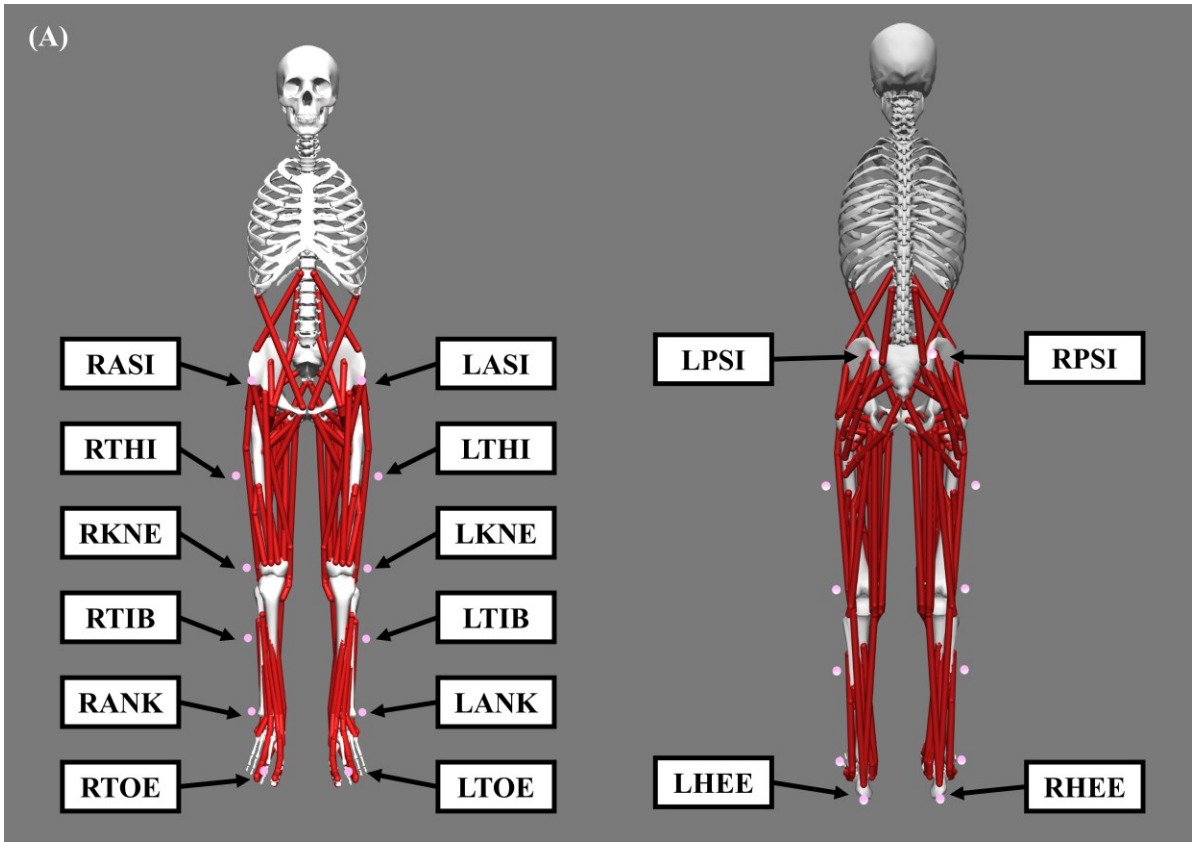

Figure 2.1 The illustration of 'gait2392' musculoskeletal model in OpenSim™ with 16 virtual markers attached based on the Helen-Hayes marker system [40].

The acronyms of 16 virtual markers show their location on the body based on the bony landmarks, starting from the pelvis to heels.

Additionally, Figure 2.2 below describes the three interested joints: hip, knee and ankle joints, all of which are shown in the flexion plane. The terminology of the joint angle is also described in this figure. For the ankle joint, taking the position of 90 degree to the tibia bone as the origin, the dorsiflexion angle is the upward bending direction, indicated by the positive angle. In contrast, the plantarflexion angle is the downward bending motion, indicated by the negative angle. Similarly, for hip joint, take upright position as the origin, the flexion angle is the positive angle, in which the leg moves forward, while the extension angle is the negative angle, in which the leg moves backward. Using similar concept, also taking upright position as the reference

point, if the knee bending backward, it is the negative flexion angle; if it is bending forward, it is the positive extension angle. Due to the human skeletal structure, unless an injury happens, the knee rarely goes to the extension position, usually less than 2-3 degree in extension angle [42].

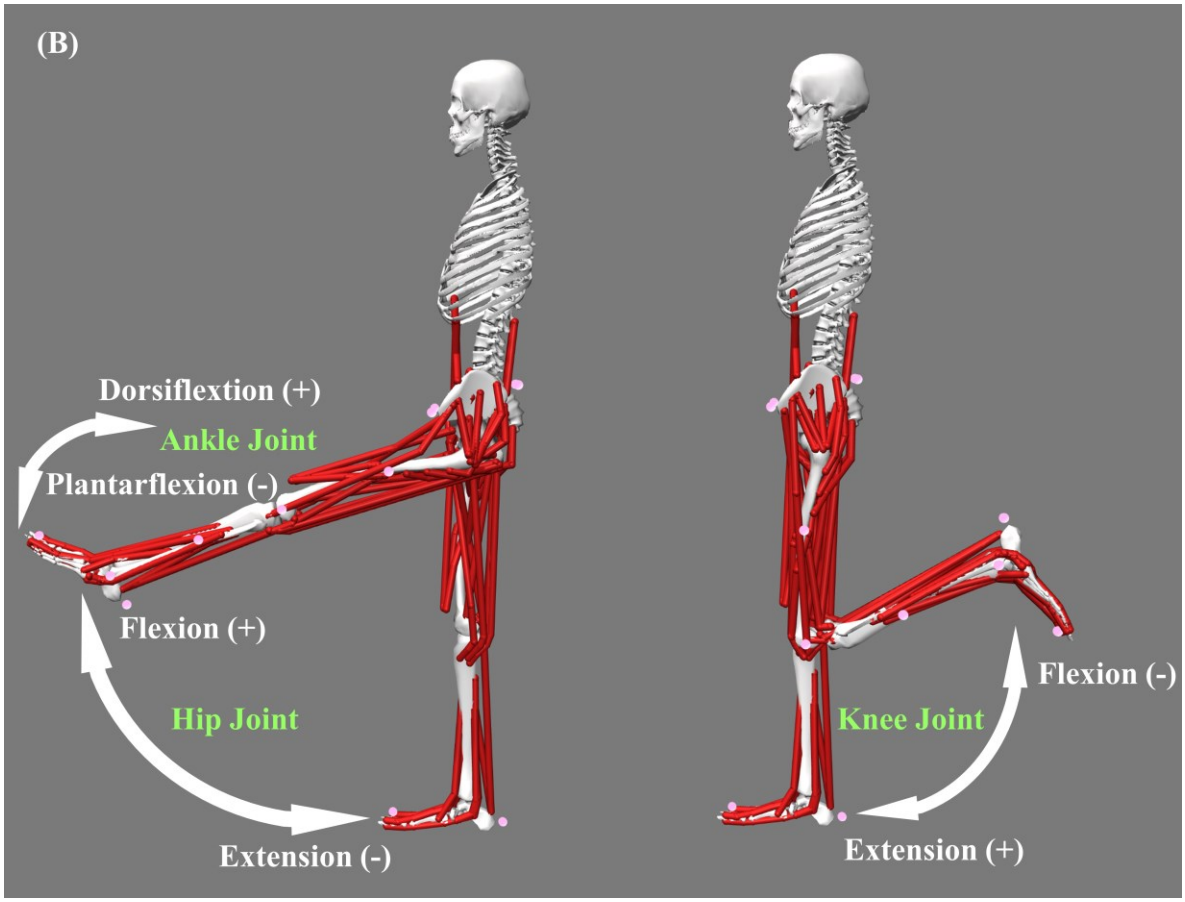

Figure 2.2 The illustration of 'gait2392' musculoskeletal model in OpenSim™ with the definitions and terminologies for joints angles of hip, knee, and ankle joints [40].

For ankle joints, positive angle is dorsiflexion motion, negative angle is plantarflexion motion.
For knee joints, positive angle is extension motion, negative angle is flexion motion.
For hip joints, positive angle is flexion motion, negative angle is extension motion.

2.3 OpenSim™ Simulation

There are four different steps to generate an accurate gait simulation in OpenSim™. In step 1, the human musculoskeletal model was scaled to match the anthropometry of an individual

subject [24]. Specifically, as shown in **Equation 2.1**, a scaling factor (s_i) was computed by dividing the relative distance (e_i) between pairs of markers obtained from the motion capture system and its corresponding virtual markers located on the model (m_i). In **Equation 2.2**, the average scaling factor (s_{avg}), which is the mean of all segments' scaling factors, can be used in case the difference between the experimental and virtual pair of markers are too large. The mass properties for each body segment were also included to scale and preserve the actual mass of the subject proportionally. Moreover, the lengths of muscle fiber and tendon were independently changed based on the scaling factors so that the overall percentage of each segment on the actuators remained the same. In this step, the input data will be the participant's body weight, the virtual marker system as well as the experimental marker trajectories. The result will be a scaled musculoskeletal model that match the specific participant.

$$s_i = \frac{e_i}{m_i} \tag{2.1}$$

$$s_{avg} = \frac{1}{n}\sum s_i \tag{2.2}$$

Next, step 2 involves extracting data using Inverse Kinematics (IK) and Inverse Dynamics (ID). By definition, kinematics is the study of motion without considering the forces and moments that produce that motion. Hence, Inverse Kinematics is the process that computes the joint angles for a musculoskeletal model that best reproduce the motion of a subject. By using the marker trajectories from the motion capture system, the IK tool in OpenSim™ was applied to identify the generalized coordinate values, consisting of joint angles and translations, that best recreate the raw marker data taken from the motion capture [24]. Mathematically, step 2 was formulated as a least-squares optimization problem that minimizes the differences between

the measured marker locations and the virtual marker locations while subjecting to the joint constraint pre-defined in the musculoskeletal model. Therefore, for each frame in the experimental kinematics, OpenSim™ would minimize a particular weighted squared error equation (shown in A.1) and calculate the optimal locations for each virtual marker for each frame in the experimental kinematics. Thus, the generalized coordinate trajectories (joint angles) can be calculated and also stored in a motion file (.MOT).

After that, the Inverse Dynamics is performed. It is defined that dynamics is the study of motion and the forces and moments that produce that motion, in which the estimation of mass and inertia is required. Therefore, in Inverse Dynamics, OpenSim™ estimates the forces and moments that cause a particular motion taken from IK step. To be more specific, an ID tool, which used the computed joint angles together with the experimental ground reaction forces and moments, was also utilized to determines the generalized forces (e.g., net forces and torques) at each joint responsible for a given movement [43]. By combining the given kinematics data describing the movement of the model and the external loads applied to it, the ID tool used this information to execute an inverse dynamics analysis. As a result, OpenSim™ can estimate the net forces and torques at each joint which produced the movement for all DOF on the model. These results could be used later to infer how muscles were utilized in a particular motion.

Even with the use of IK and ID tools, the measured reaction forces and moments were often dynamically inconsistent with the model kinematics due to the experimental error as well as the modeling assumptions. Therefore, step 3 in OpenSim™'s workflow, called residual reduction algorithm (RRA), focused on optimizing the computed generalized coordinates in the previous steps to be dynamically consistent with the experimental inputs [24]. This was done by reducing the residual forces and moments in the Modified Newton's second law equation (A.2),

which presented the relationship between the measured ground reaction force, gravitational acceleration, and the accelerations of the body segments [24]. In this case, the residual was defined as the effects of modeling and marker processing errors that accumulated gradually and led to a large nonphysical compensatory forces [17,44]. Specifically, to reduce the residual forces and moments, the average values of these residuals at each actuator were calculated over the duration of the movement. Then, the RRA modified the model mass parameters (center of mass locations, etc.) based on these averages, aiming to decrease the average values of the residuals. This can be done by altering the torso mass center of the body (i.e. to correct the excessive leaning due to inaccuracies in mass distribution and geometry of the torso) and redistributing a desired mass change (computed from the residual forces) proportionally among body segment [24,25]. These adjustments would affect the initial joint kinematics of the musculoskeletal model, making it consistent to the experimental ground reaction forces and torques while maintaining the accurate and desired biomechanical results. Moreover, an upper limit could also be applied by the users on the magnitudes of the residuals to reduce the computational cost and simulation time.

Lastly, in step 4, the computed muscle control (CMC) tool in OpenSim™ was used to analyze and create a set of muscle excitations that drove the generalized coordinates of a dynamic musculoskeletal model towards the desired kinematic movement [45]. CMC did this by using a combination of proportional-derivative control and a static optimization criterion to distribute forces across synergistic muscles and establish a forward dynamic simulation that matched the adjusted kinematics movement taken from the previous step [24,45]. Notably, in OpenSim™, static optimization (SO) tool is an extension from ID that further use the known net joint moments to solve for the unknown individual muscle forces at each instant in time by

minimizing the sum of squared muscle activations. The SO can either use the input from IK or from RRA results. If the IK input is used, it needs to go through a Butterworth lowpass filter (6Hz by default) to reduce the noise; while the RRA result can be use as it is. The SO will then compute and store the time history of the muscle activation and force to analyze human postural adjustments in quick manner. Thus, depending on the size of the dataset, SO tool can be used separately to extract muscle force data and reduce the simulation runtime.

On the other hand, CMC tool, which is an enhanced, more complex version of SO, occupied much higher computational resources comparing to the other tools in OpenSim™, causing it to be used on small and specific time frames of interest rather than applying on the whole simulation [26]. The procedure of CMC tool started with the estimation for a set of desired accelerations that could drive the model coordinates toward the experimentally-derived coordinates [46]. Since the forces that muscles apply to the body cannot change instantaneously, the desired accelerations computed with the CMC tool must be generated in a small time step T [46]. This time step T was often determined to be 0.01 seconds for musculoskeletal model as it not only was short enough for adequate control but also long enough for muscle force modification [45]. Then, the actuator control needed to achieve the desired accelerations was calculated in term of muscle excitation or fiber force. This led to the use of static optimization to allocate the loads across synergistic actuators in the model [46]. Finally, the CMC algorithm conducted a standard forward dynamic simulation, advancing the analysis forward in time by T. The dynamics simulation was modeled by relating the time rate of change of muscle activation to muscle activation and excitation, whose equation is shown A.3 [24]. All the earlier steps—computing the desired accelerations, static optimization, and forward dynamic simulation—were repeated until time was advanced to the end of the desired movement interval, designated by the

user. After these steps, the results of the simulation were either plotted in OpenSim™ or exported to other statistical processing software for further analysis.

CHAPTER III

RESULTS

3.1 Joint Angles

Figure 3.1 below illustrates the joint angles of the hip, knee, and ankle during the time period of interest for 18 participants under all reported trials with different slippery conditions. Comparing to the normal gait condition, the patterns of the other three cases change with respect to the increase in slippery perception of the participants. Particularly, the participants appeared to intentionally alter their gait postures to prevent the slip event from happening. Moreover, there are some fluctuations in angle for most of the slippery cases, especially in US trials, all of which represent the occurrence of slip events as well as potential falls during the experiments. As the participants lose their balance due to the slips, their body will perform a series of corrective movements that affect the joint angles, joint moments, and all of their associated muscle groups, resulting in the fluctuation in the recorded gait data. The reported average values for all the gait trials in 0 below also show the joints and muscle corrective movements.

Table 3.1 The average angle values of hip, knee and ankle joint under different gait conditions in three phases.

Avg. Angle (Degree)	Hip			Knee			Ankle		
	Phase 1	*Phase 2*	*Phase 3*	*Phase 1*	*Phase 2*	*Phase 3*	*Phase 1*	*Phase 2*	*Phase 3*
NG	12.77	-14.68	-27.83	-12.01	-10.22	-27.32	-4.55	7.39	1.10
US	11.34	-15.67	-29.24	-11.04	-9.39	-27.93	-6.42	4.43	-2.56
AS	11.67	-15.25	-30.47	-11.18	-10.02	-24.73	3.10	13.12	5.57
ES	10.74	-16.77	-28.48	-10.36	-9.69	-31.10	1.58	12.99	2.55

The average joint angles data are recorded based on each joint (column), phases (sub column), and gait condition (row).

These results describe how the body alter its posture depending on the slip perception. Taking the angle at phase 3 of the ankle joint as an example, the foot is in 1.1° dorsiflexion angle in normal gait, then it decreases into 2.56° plantarflexion angle in US trial. This shows most of the participant did slip in this trial and try to bend down the ankle as a mean to grip the ground and maintain balance, which is a common behavior of the body during a slip event [47]. Then, for the next AS trial, even though they were told that they might or might not slip, the participants still got scared and overcompensated their gait posture, making it stiffer and resulting in over 5 degree in dorsiflexion (bending upward) during toe off phase. Finally, for ES trial, since they knew exactly that they were about to slip, their body got relaxed and tuned in their corrective movement just enough to sustain their balance, as shown in the 2.55° dorsiflexion angle in 0. Similar pattern can be seen in Phase 1 and 2 of the ankle's joint angle. These data not only confirm how the body try to recover from a slip event in US trial but also clearly illustrate its corrective movement during AS and ES trial due to an increase in slip perception.

To be more specific, in Phase 1 (heel strike), the AS and ES slippery conditions have higher flexion angles at the knee joints (10%) as well as higher dorsiflexion angles at the ankle joints (80%) compared to the dry condition. Especially, the hip flexion angles are smaller in

these two slippery trials as compared to the normal gait (around 15% smaller in average). This change leads to a smaller and shorter stride in the gait pattern of participants under slippery condition, which describes one of the corrective movements of their body to keep balance as well as to prevent the slips. Additionally, an increase in hip extension of the slippery trials, as shown in Phase 2 and 3, indicates that the leg stayed on the ground longer during the midstance phase of the task duration, leading to a boost in gait stability of the participants. In contrast, knee joints showed an increase flexion angle to its dry-condition counterpart, at approximately 5%. These results mean that, unlike hip joints, the knee joint still maintains its function of preserving the gait pattern while maintaining a strong support that connects the upper to the lower extremities during gait under slippery conditions. Furthermore, the ankle joints' angles yielded the largest change regarding magnitude when compared to the normal gait data, with a change from plantarflexion to dorsiflexion in Phase 1, then followed by the increase of 70% and 120% in dorsiflexion angles in Phase 2 and 3, (-4.55 to 1.58 degree, 7.39 to 12.99 degree, 1.1 to 2.55 degree, respectively). These large changes in the angles of ankle joints shorten the range of motion of the ankle, making it stiffer and leaning the body backward during the gait as compared to the normal gait pattern. Therefore, this adjustments in body posture keeps the center of mass of the upper body falling into a range of support of the lower limbs, aiming to sustain the stability of the human body.

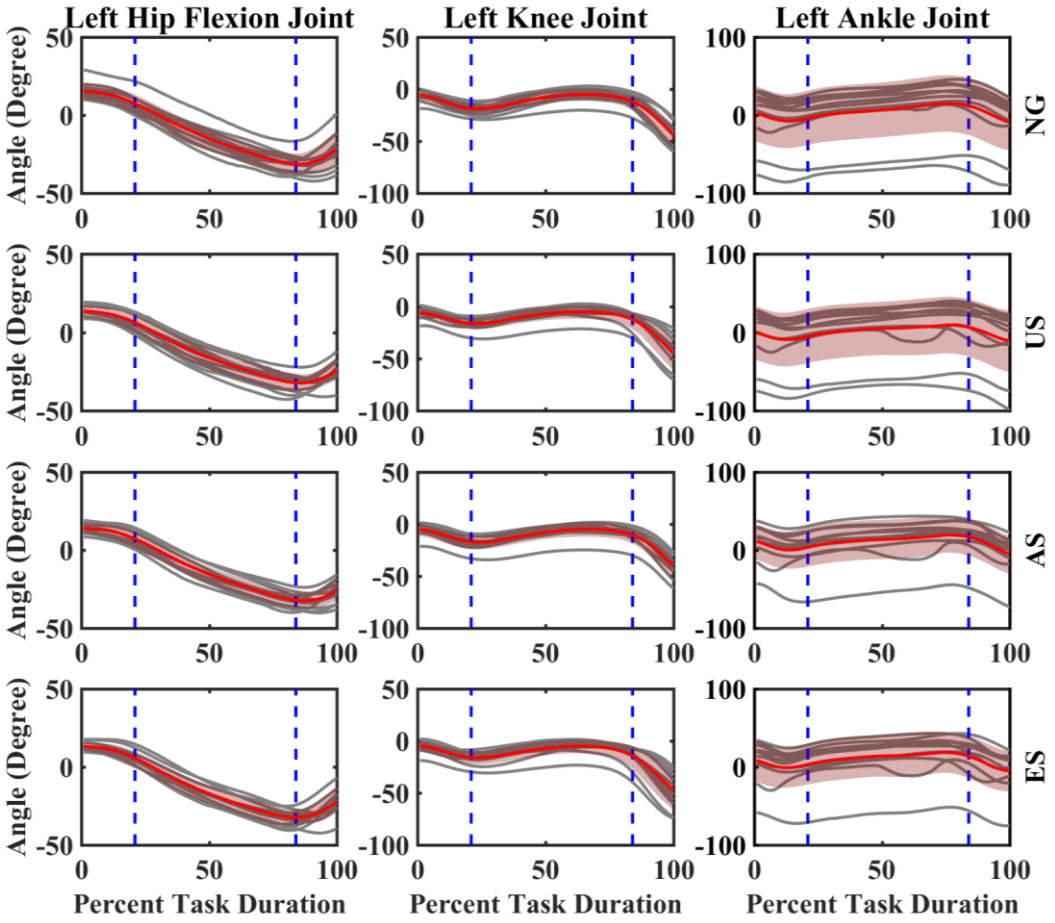

Figure 3.1 The joint angles of left hip, knee, and ankle joints of the participants during the time period between the left heel strike and toes off phase during each of the four slippery conditions.

The gray lines show results for each of the participant while the red line indicates the average value of all participants in a particular trial, followed by a red-shaded region that represents the standard deviation of the average value during the task duration. The blue-dotted lines separate the task duration into Phase 1, Phase 2 and Phase 3.

Another approach to identify possible corrective movements of the body is to analyze and compare the joint angles and moments among the three slippery conditions. Particularly, the ankle joint gait data under AS and ES condition is significantly larger from that of the US condition. Opposite from the US trial, the ankle joints of the AS and ES trial had a slight increase

in dorsiflexion in Phase 1 and a sharp increase dorsiflexion in angles in latter phases. The influence of the slip perception had altered the gait posture of the participants during an alerted and expected slip events, which not only raises the coefficient of friction among the foot-floor interface, but also reduces the fluctuation of the center of mass, keeping the center of mass closer to the body's line of gravity and thereby ensuring the balance of the gait cycle. Furthermore, knee joint angles do not have any remarkable changes among the three slippery trials (less than 5%). The largest change in the knee joint occurs in the flexion angle and increase as the slip perception of the participants increase. This transformation in gait data means that the knee is stiffer than the NG trials in order to reduce the generated moment at the knee joints, stabilize the center of mass, and support the upper half of the body to alleviate the risk of falling. Likewise, while having a minor rise in extension angles, the hip joint angles in ES trials are smaller in term of flexion angle (15% different), which result in a shorter stride comparing to US trials. Overall, among the three gait trials under distinct slippery condition, the knee joints' angles tend to be fixed for body support while the ankle joints adapt and adjust the angle to reduce the moment, increase the friction force with the floor, and stabilize the body's center of mass. Meanwhile, the hip joints are only varied slightly and responsible for accommodating the postural change by aiding the ankle joints in balancing the upper body.

3.2 Joint Moments

Additionally, the effect of the slippery conditions can be illustrated using the data of joint moments in Figure 3.2 and Table 3.2. In general, the joint moments at three joints during three slippery conditions are smaller comparing to that of the dry condition. Among the three slippery trials, the AS cases yielded the largest joint moments comparing to the US and ES cases, which is corresponding to the overcompensation of the body movement after experiencing a slip event

in the prior US trial. These results also prove that, as the perception for slip propensity increases, the body produces less torques as a corrective response to the slippery environment in order to maintain a strong support for the upper body as well as stable the center of mass of the core. Moreover, the data of the hip, knee and ankle from Table 3.2 clearly describes this decline in joint moments. For example, hip moments in Phase 1 during ES condition (14.91 N.m) are significantly smaller than that of the NG, US and AS cases (53.19 N.m, 23.06 N.m, 25.31 N.m, respectively). When comparing the joint moments among the three slippery cases, ES case also have the smallest moments at all joints, which directly link to the participant's increase in awareness of the slippery floor.

Table 3.2 The average moment values of hip, knee and ankle joint under different gait conditions in three phases.

Avg. Moment (N.m)	**Hip**			**Knee**			**Ankle**		
	Phase 1	***Phase 2***	***Phase 3***	***Phase 1***	***Phase 2***	***Phase 3***	***Phase 1***	***Phase 2***	***Phase 3***
NG	53.19	293.23	254.05	102.26	280.27	209.63	122.05	221.68	136.12
US	23.06	247.46	195.17	76.16	236.44	154.03	101.38	180.91	93.32
AS	25.31	269.51	256.59	79.30	258.22	209.23	105.32	196.39	130.21
ES	14.91	249.45	200.74	63.35	231.92	160.16	87.91	170.22	95.21

The average joint moments data are recorded based on each joint (column), phases (sub column), and gait condition (row).

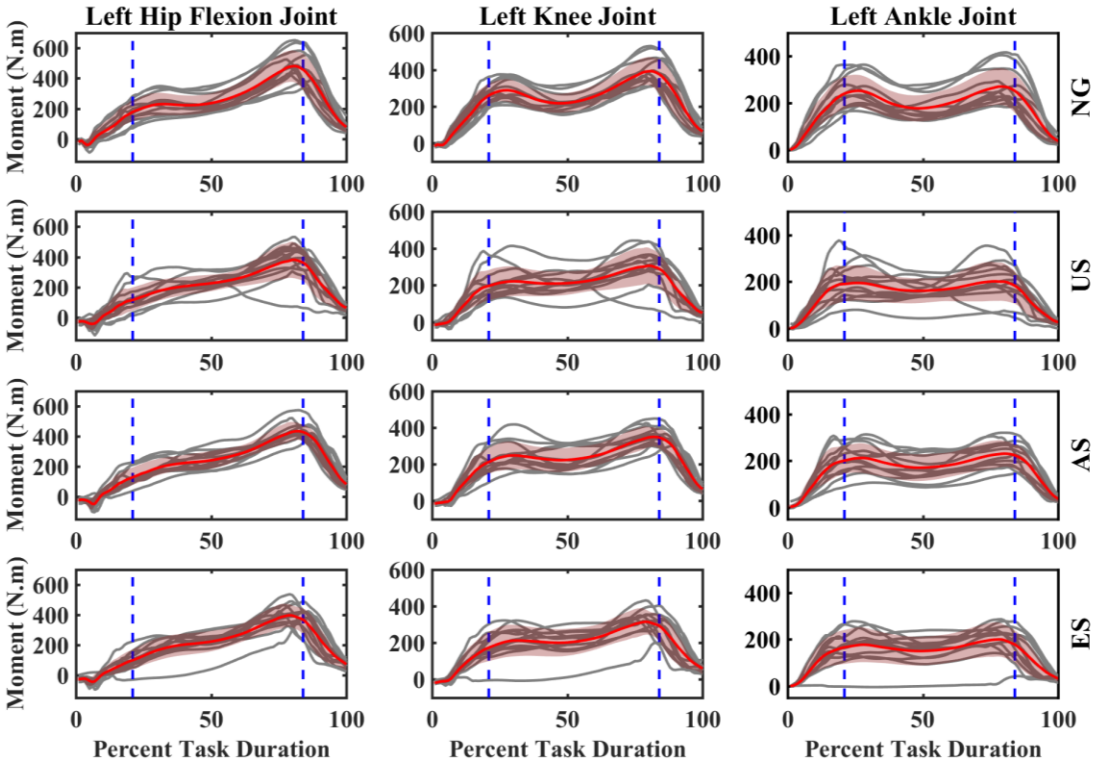

Figure 3.2 The joint moments of left hip, knee, and ankle joints of the participants during the time period between the left heel strike and toes off phase during each of the four slippery conditions.

The gray lines show results for each of the participant while the red line indicates the average value of all participants in a particular trial, followed by a red-shaded region that represents the standard deviation of the average value during the task duration. The blue-dotted lines separate the task duration into Phase 1, Phase 2 and Phase 3.

Notably, the US gait trials as shown in Figure 3.2 often contain higher knee extension angles and ankle plantarflexion angles, which proves the occurrence of a slip events in these trials. When slips happen, the foot of the participant will slide on the slippery floor and may induce falls, leading to an increase in knee and ankle joints angles. An unexpected slip event also accompanies by an uncontrolled muscle response prior to the slip incident, which was shown by the smaller joint moments in US trials. This means that, without the knowledge of the slip surface, the body would not have any corrective responses to increase its control over the muscle

groups in the lower extremity. However, these patterns can be reduced by raising the participants' perception of the slippery floor. The effect of perception can be proved by using the joint angles and joint moments data of ES trials, in which all the participants had the knowledge about the slippery surface that they would walk on. In this case, the results from ES trials of all three joints show restricted joint angles, lower joint moments and declined range of motion, which represents the body adjustment of the gait pattern in order to maintain the balance as well as prevent the slips.

3.3 Muscle Forces

Similarly, the fiber forces extracted from the gait trials also describes the body's postural adjustments through different groups of muscle to preserve balance and avoid falling. Figure 3.3 consecutively demonstrate the fiber force of four prime-mover groups of gait trials under three slippery conditions as well as normal environment. Additionally, the average fiber force values of each of the prime-mover groups are also computed and reported in Table 3.3. Among the four muscle groups, the fiber forces of TA and VI yield the most fluctuation across different trials. However, this pattern starts to decrease as the slip perceptions of the participants increase in the following slippery trials. Besides, there are considerable fluctuations of force magnitudes in Phase 1 and Phase 3 of task duration in all the slippery trials, especially the US condition. These trends of rapidly increasing fiber force (for TA and VI) or decreasing fiber force (for BF and MG) around the beginning and the end of the task duration illustrate the influence of slip events on the gait cycle of the participant. These trends also explain the similar pattern seen in the fiber force data of AS and US trials, in which slips occurred and altered the magnitude of the fiber force in the prime-mover muscle groups. The magnitudes of fiber forces in ES trials are generally smaller and more balanced compared to the other two slippery trials, which indicates

the response from the body's corrective movements in the attempt to maintain postural stability under the impact of slippery surface.

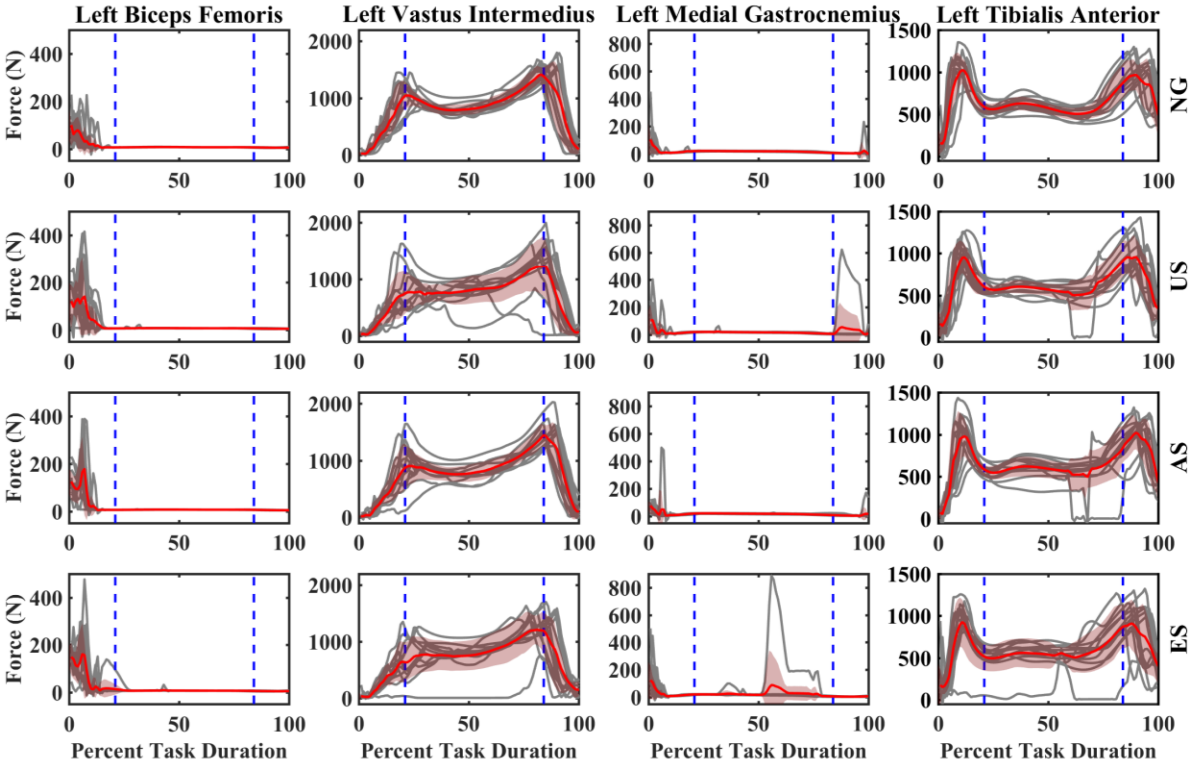

Figure 3.3 The fiber forces of the four prime-mover muscle groups of the participants during the time period between the left heel strike and toes off phase during NG, US, AS and ES conditions.

Gray lines – participants' fiber force values, red line – average value of all participants, red-shaded region – corresponding standard deviation, blue-dotted line – indicate ending of Phase 1 and Phase 2.

Table 3.3 The average fiber force values of the four prime-mover muscles under different gait conditions in three phases.

Avg. Force (N)	Biceps Femoris (BF)			Vastus Intermedius (VI)		
	Phase 1	***Phase 2***	***Phase 3***	***Phase 1***	***Phase 2***	***Phase 3***
NG	30.34	6.35	4.68	416.16	960.75	743.89
US	59.45	6.32	4.45	330.63	872.00	538.74
AS	53.80	6.21	4.43	336.36	913.89	794.18
ES	62.74	6.67	4.45	287.67	862.26	574.40

Table 3.3 (continued)

Avg. Force (N)	Medial Gastrocnemius (MG)			Tibialis Anterior (TA)		
	Phase 1	***Phase 2***	***Phase 3***	***Phase 1***	***Phase 2***	***Phase 3***
NG	21.44	16.42	5.47	697.51	590.64	827.39
US	26.03	16.10	29.46	632.79	599.32	741.72
AS	22.65	16.75	6.59	630.19	597.33	834.55
ES	29.32	27.38	4.51	580.89	567.44	724.14

The average muscle forces data are recorded based on each joint (column), phases (sub column), and gait condition (row).

The TA muscle, associated with dorsiflexion ankle joints, and VI muscle, associated with extension knee joints, has a greater change in force magnitudes compared to the other muscles, especially in Phase 1 and Phase 3. The TA and VI muscles were utilized to push the body forward during the stance phase, in which they generated forces and moments to counter the ground reaction force resulted from the interaction between the foot and the ground. The slight decreases in magnitude of TA and VI muscles (10-30% decrease) show the body's postural adjustment to stabilize gait under slippery condition. Alternatively, the MG muscle (associated with plantarflexion ankle joints) and BF muscle (associated with flexion knee joints) have a minimal change in force magnitudes, which is due to the limited use of plantarflexion ankle joints and flexion knee joints during the stance phase of a gait cycle [38]. According to **Figure 3.3**, BF and MG are utilized during the Phase 1 of the task duration (heel strike), when the heel

touched the ground and the muscles were recruited to maintain postural stability as well as generate enough forces and moments to roll the foot onto the surface (entering midstance). However, there is an exception in the muscle force of MG at Phase 3 during US trials. The sharp increase in MG muscle forces in Phase 3 (toe off) represents an initiation of a slip event due to the slippery surface. In this case, the participants tried to maintain their posture by bending the ankle downward to grab the ground with their toes and increase the coefficient of friction of the foot-floor interface, thus, utilizing MG muscle to perform plantarflexion motion at the ankle. These results are correlated to the joint angle and joint moment values as they match the responsiveness of each joint when being subject to the corrective movements of gait postures under slippery conditions. When comparing the fiber forces of the slip trials among each other, a similar result with the joint angles analysis can be derived. To be more specific, the magnitudes of the fiber forces tend to get smaller as the slip perceptions of the participants increase. This result can be seen in the force values of BF and VI, which describes the responses of hip and knee joints to the corrective movements of the body. This means the knee joints reduce the moment and become stiffer supports for the body, while hip joints slightly adjust the stride to accommodate the postural change and stabilize the upper body.

In contrast, even though there are some errors in a few trials during data collection process, the extracted fiber force of MG and TA rises proportionally to the participants' perception of slips (in AS and ES trials). This result proposes that, as their perceptions for a potential slip increase, the participants tend to put more control on their ankle joints to preserve their balance in the form of leaning backward to minimize the body center of mass excursions outside the base of support of the lower limbs or reducing angular velocity to increase the coefficient of friction between the foot-floor interface. Notably, this frequent use of TA muscle

over other prime-mover muscles to balance the body during gait under slippery conditions might pose a potential site of injury around TA muscle, which can also be one of the reasons that explain the typical ankle-related injuries due to STFs.

CHAPTER IV

DISCUSSION

The purpose of this study was to analyze and extract the biomechanical variables of joint kinematics and muscle activities of the slipping leg during slip initiation of participants when exposed to dry gait, unexpected, alerted, and expected slips using OpenSim™ musculoskeletal computational models and simulations. These simulations reveal significant interactions between slip perceptions of participants and the biomechanical variables attained from OpenSim™ in terms of joint angles and fiber forces. On average, greater plantarflexion angle and greater muscle forces (VI and TA) were seen on the ankle-related joints and muscles, which support the previous findings of Chander et al. [11,35]. Knee and hip joints, in contrast, showed no significant results comparing to the ankle joints at heel strike. This result proposed that, at heel strike, the modifications of gait posture in the lower body appeared to be affected mainly by the distal ankle joints, while the knee and hip joints did not leave any remarkable influence on the gait adjustment until post heel strike.

This finding supports a previous study of Chander et al. that during a slip event, the ankle joint attempted to go further in plantarflexion angle to prevent the slips while the knee and hip joints was forced into a smaller amount of flexion as the lower limbs was abruptly sliding toward the anterior direction [11]. Specifically, the greater plantarflexion during slip events taken from the OpenSim™ analysis supported a study from Shroyer et al., which indicated this increased plantarflexion angle was a recovery mechanism of the body to maintain balance by gripping the

footwear using the toes [48]. Moreover, the greater plantarflexion ankle angle during slip trials could also be seen as an attempt to make contact with the floor in a flatter foot position to extend the contact surface area of the foot, thereby preventing the occurrence of slips [6,14].

Furthermore, the muscle activities from the lower extremity that involves in the reactive response of the human postural control system also play an important role during a slip and for an impending slip [11]. A muscle activation pattern study under slippery conditions by Chambers et al. suggests an increased power of the TA muscle, as well as duration, was noted during hazardous slips as an attempt to achieve flat-foot, an important aspect in slip recovery and continuation of gait [15]. Based on the activation of the medial hamstring, medial gastrocnemius and vastus lateralis (corresponding to BF, MG, and VI in this case), Chambers et al. also identified two detrimental effects on balance recovery and gait cycle progression: (a) delayed anterior movement of the body COM over the base of support, and (b) knee buckling—decreased knee extension in stance to prevent fall. The fiber force results extracted from OpenSim™ did support the previous literature findings in Chambers et al.'s work [15]. Additionally, the muscle force values of the prime muscle groups are also supported by the data in Heintz et al. studies [49]. In this study, Heintz and her team utilize EMG data to compute muscle force during normal gait using static optimization algorithms. The forces of various muscle groups were computed and Heintz's results are closely corelated to the data in **Figure 5** and **Table 3**.

The last factor that affects the body corrective movement in response of an impending slip events is the perception of a slip hazard. There are several elements that have impact on the slip perceptions such as the prior knowledge of a slip-prone environment, the visual perception in the presence or absence of lighting and the mental workload of the participants [50]. According to previous literature, the anticipation of slippery floor allowed the

participant to the reduce potentials slip events by adjusting the biomechanics of gait [19,47]. These gait adaptations consisted of a reduction in foot-floor angle to create a more flat foot position at heel strike [5], the minimization of normal and shear forces during stand phase [6], all of which lower the frictional requirements needed to prevent slips. These findings are similar to the results from the joint angles and fiber forces derived from OpenSim™. As the participants' perceptions of the slip increased, the ankle joints had lower dorsiflexion and higher plantarflexion angles, which hindered the body from leaning forward and reduce the fluctuation of the center of mass, resulting in a more stable gait pattern ranging from US to AS to ES trials. As a result, using the data extracted from OpenSim™, it can be concluded that the knowledge and the anticipation of the slippery flooring surface was crucial in the modification of gait pattern that controlled by the human anticipatory postural control system, thereby preventing slips and slip-induced falls.

Besides the ability to extract hard-to-identify data from experiments, there are several other applications of OpenSim™ in the analysis of gait and human biomechanics. One of the most promising potential of OpenSim™ is the ability to perform various 'what-if' studies to test hypotheses and predict the functional outcome such as emergent behaviors or injury threshold [17]. OpenSim™ simulations can be used to identify new movements and establish the relationships between different posture, muscle forces, joint angle, and ground reaction force, all of which enable researchers to more readily use predictive simulation as a tool to address clinical conditions that limit human mobility [51]. Moreover, OpenSim™ can also be utilized to facilitating the interactions between modelers and experimentalists [24]. Precisely, modelers need experimentalists to acquire parameters used in simulations as well as data to validate the simulation results. Conversely, experimentalists can benefit from the interpretation of modelers

on the biomechanical experiments in term of theoretical framework, data analysis and the need for improved experimental protocols. For example, OpenSim™ can be treated as an analysis tool in athletic training and medical rehabilitation by integrating the human biomechanics into musculoskeletal models to assess, predict, and mitigate injury risk of athletes or patients under various circumstances. If coupled with high-quality experimental measurements, subject-specific simulations on OpenSim™ can help elucidate how elements of the neuromusculoskeletal system interact to produce a suitable movement for athletes or to improve the outcomes of treatments for patients with movement disorders [24,27,34]. Therefore, it can be concluded that the accuracy of a simulation firmly depends on the fidelity of the underlying mathematical models of the musculoskeletal system and its corresponding assumptions based on limited experimental evidence [25].

To improve the accuracy of the current OpenSim™ simulations on gait under slippery conditions, a complex musculoskeletal model with a larger number of muscles, joints and degree of freedoms is needed to fully capture the whole-body movements and its corrective movement in response of the slippery conditions. A different marker system with larger number of markers is also needed, especially for the upper body, as they can stabilize the musculoskeletal model during data extraction process, which not only can reduce the marker errors but also boost the runtime of the simulation, enhance the accuracy of the result and track the gait cycle more efficiently. Moreover, the lengths of major body segments of the participant (femur, tibia, etc.) are needed in future study to improve the musculoskeletal model scaling process in OpenSim™. For this study, the average scaling factor was used for all participants to scale their body segments onto the model. Since different participants have different segment dimensions, using a generalized ratio in scaling might affect the lengths of the muscle groups attached to a body

segment, which eventually alter the maximum fiber forces that they can produce. Lastly, to further improve the simulation results from OpenSim™, an updated list of muscle properties is needed. Currently, the musculoskeletal model used in this study ('gait2392') utilized the muscle foundation (such as muscle fiber length, tendon length, max isometric force, pennation angle, contraction velocity, etc.) from Delp et al. to drive the simulation and calculate its result [52]. However, since these muscle properties are collected from cadaveric experiments during the 1990s, which was outdated and also different from the muscles of living beings, a clinical study using current technology should be performed to identify and collect these muscle properties to advance the medical and biomechanical studies on the human body. If such a muscle properties is integrated with OpenSim™, the simulation results will be improved significantly and the connection between human muscles/tendons/ligaments with biomechanical injuries and failures can be investigated thoroughly.

CHAPTER V

CONCLUSION

The current study uses OpenSim™ musculoskeletal models and simulations to analyze the slips and trips gait data under slippery conditions. The participants were exposed to dry gait, unexpected, alerted, and expected slips, then various biomechanical variables, pertinent to injury biomechanics, that are not experimentally measured were obtained (muscle activations, muscle forces, joint angles and moments). The motion capture gait data from Chander et al. [11,34] was imported into OpenSim™, then data of the hip, knee and ankle join angles, as well as the fiber force of four primary muscle groups (BF, MG, VI, TA) were extracted and post-processed in MATLAB™.

In general, during the slip process, the joint angles of the plantarflexion ankle increase to preserve the traction between the lower extremity and surface, and thus the friction force with the floor, to stabilize the body's center of mass and reduce the slip movement. Meanwhile, the joint angles of the knee were shown to be fixed to support the body, and the hip joint angles slightly adjusted to balance the upper body as well as accommodate the postural change. These results agree with what have been found in previously published studies. Overall, the project provides a practical alternative method to extract biomechanical variables of various muscles and joints during slip movements that are difficult to measure. This is also the first study that utilizes OpenSim™ to analyze gait data under slippery conditions. Hence, the study will aid in the prediction of injury thresholds and location for slip-trip, as well as identify new movements and

relationships among muscle forces, joint angles and posture, which can be further applied to predict and reduce injury risks in clinical or athletic training conditions.

REFERENCES

[1] 2018, “Census of Fatal Occupational Injuries (CFOI) - Current and Revised Data,” US Dep. Labor, Bur. Labor Stat. [Online]. Available: https://www.bls.gov/iif/oshcfoi1.htm#2018. [Accessed: 19-Oct-2020].

[2] Davis, P. R., 1983, “Human Factors Contributing to Slips, Trips and Falls,” Ergonomics, **26**(1), pp. 51–59.

[3] Gauchard, G., Chau, N., Mur, J. M., and Perrin, P., 2001, “Falls and Working Individuals: Role of Extrinsic and Intrinsic Factors,” Ergonomics, **44**(14), pp. 1330–1339.

[4] Redfern, M. S., Cham, R., Gielo-Perczak, K., Grönqvist, R., Hirvonen, M., Lanshammar, H., Marpet, M., Pai, C. Y. C., and Powers, C., 2001, “Biomechanics of Slips,” *Ergonomics*, Taylor & Francis Group , pp. 1138–1166.

[5] Hanson, J. P., Redfern, M. S., and Mazumdar, M., 1999, “Predicting Slips and Falls Considering Required and Available Friction,” Ergonomics, **42**(12), pp. 1619–1633.

[6] Cham, R., and Redfern, M. S., 2002, “Heel Contact Dynamics during Slip Events on Level and Inclined Surfaces,” *Safety Science*, Elsevier, pp. 559–576.

[7] McGorry, R. W., DiDomenico, A., and Chang, C. C., 2010, “The Anatomy of a Slip: Kinetic and Kinematic Characteristics of Slip and Non-Slip Matched Trials,” Appl. Ergon., **41**(1), pp. 41–46.

[8] Perkins, P. J., 1978, “MEASUREMENT OF SLIP BETWEEN THE SHOE AND GROUND DURING WALKING.,” *ASTM Special Technical Publication*, ASTM, pp. 71–87.

[9] Strandberg, L., and Lanshammar, H., 1981, “The Dynamics of Slipping Accidents,” J. Occup. Accid., **3**(3), pp. 153–162.

[10] Lockhart, T. E., and Kim, S., 2006, “Relationship between Hamstring Activation Rate and Heel Contact Velocity: Factors Influencing Age-Related Slip-Induced Falls,” Gait Posture, **24**(1), pp. 23–34.

[11] Chander, H., Wade, C., Garner, J. C., and Knight, A. C., 2017, “Slip Initiation in Alternative and Slip-Resistant Footwear,” Int. J. Occup. Saf. Ergon., **23**(4), pp. 558–569.

[12] Chang, W. R., Li, K. W., Huang, Y. H., Filiaggi, A., and Courtney, T. K., 2004, "Assessing Floor Slipperiness in Fast-Food Restaurants in Taiwan Using Objective and Subjective Measures," Appl. Ergon., **35**(4), pp. 401–408.

[13] Li, K. W., Wu, H. H., and Lin, Y. C., 2006, "The Effect of Shoe Sole Tread Groove Depth on the Friction Coefficient with Different Tread Groove Widths, Floors and Contaminants," Appl. Ergon., **37**(6), pp. 743–748.

[14] Cham, R., and Redfern, M. S., 2002, "Changes in Gait When Anticipating Slippery Floors," Gait Posture, **15**(2), pp. 159–171.

[15] Chambers, A. J., and Cham, R., 2007, "Slip-Related Muscle Activation Patterns in the Stance Leg during Walking," Gait Posture, **25**(4), pp. 565–572.

[16] Li, K. W., and Chin, J. C., 2005, "Effects of Tread Groove Orientation and Width of the Footwear Pads on Measured Friction Coefficients," *Safety Science*, Elsevier, pp. 391–405.

[17] Reinbolt, J. A., Seth, A., and Delp, S. L., 2011, "Simulation of Human Movement: Applications Using OpenSim," Procedia IUTAM, **2**, pp. 186–198.

[18] Winter, D. A., 1995, "Human Balance and Posture Control during Standing and Walking," Gait Posture, **3**(4), pp. 193–214.

[19] Lockhart, T. E., Spaulding, J. M., and Park, S. H., 2007, "Age-Related Slip Avoidance Strategy While Walking over a Known Slippery Floor Surface," Gait Posture, **26**(1), pp. 142–149.

[20] Brady, R. A., Pavol, M. J., Owings, T. M., and Grabiner, M. D., 2000, "Foot Displacement but Not Velocity Predicts the Outcome of a Slip Induced in Young Subjects While Walking," J. Biomech., **33**(7), pp. 803–808.

[21] Moyer, B. E., Chambers, A. J., Redfern, M. S., and Cham, R., 2006, "Gait Parameters as Predictors of Slip Severity in Younger and Older Adults," Ergonomics, **49**(4), pp. 329–343.

[22] Madadi-Shad, M., Jafarnezhadgero, A. A., Sheikhalizade, H., and Dionisio, V. C., 2020, "Effect of a Corrective Exercise Program on Gait Kinetics and Muscle Activities in Older Adults with Both Low Back Pain and Pronated Feet: A Double-Blind, Randomized Controlled Trial," Gait Posture, **76**, pp. 339–345.

[23] Jafarnezhadgero, A. A., Majlesi, M., Etemadi, H., Hilfiker, R., Knarr, B. A., and Madadi Shad, M., 2020, "Effect of 16-Week Corrective Training Program on Three Dimensional Joint Moments of the Dominant and Non-Dominant Lower Limbs during Gait in Children with Genu Varus Deformity," Sci. Sport., **35**(1), pp. 44.e1-44.e11.

[24] Delp, S. L., Anderson, F. C., Arnold, A. S., Loan, P., Habib, A., John, C. T., Guendelman, E., and Thelen, D. G., 2007, "OpenSim: Open-Source Software to Create and Analyze Dynamic Simulations of Movement," IEEE Trans. Biomed. Eng., **54**(11), pp. 1940–1950.

[25] Seth, A., Sherman, M., Reinbolt, J. A., and Delp, S. L., 2011, "OpenSim: A Musculoskeletal Modeling and Simulation Framework for in Silico Investigations and Exchange," *Procedia IUTAM*.

[26] Uchida, T. K., Seth, A., Pouya, S., Dembia, C. L., Hicks, J. L., and Delp, S. L., 2016, "Simulating Ideal Assistive Devices to Reduce the Metabolic Cost of Running," PLoS One, **11**(9), pp. 1–19.

[27] Marieswaran, M., Sikidar, A., Goel, A., Joshi, D., and Kalyanasundaram, D., 2018, "An Extended OpenSim Knee Model for Analysis of Strains of Connective Tissues," Biomed. Eng. Online, **17**(1), pp. 1–13.

[28] Catelli, D. S., Wesseling, M., Jonkers, I., and Lamontagne, M., 2019, "A Musculoskeletal Model Customized for Squatting Task," Comput. Methods Biomech. Biomed. Engin., **22**(1), pp. 21–24.

[29] Xu, H., Bloswick, D., and Merryweather, A., 2014, "An Improved OpenSim Gait Model with Multiple Degrees of Freedom Knee Joint and Knee Ligaments," Comput. Methods Biomech. Biomed. Engin., **18**(11), pp. 1217–1224.

[30] Kim, H. K., and Zhang, Y., 2016, "Estimation of Lumbar Spinal Loading and Trunk Muscle Forces during Asymmetric Lifting Tasks: Application of Whole-Body Musculoskeletal Modelling in OpenSim," Ergonomics, **60**(4), pp. 563–576.

[31] Phan, P., Vo, A., Bakhtiarydavijani, A., Burch, R., Smith, B. K., Ball, J. E., Chander, H., Knight, A., and Prabhu, R., 2021, "In Silico Finite Element Analysis of the Foot Ankle Complex Biomechanics: A Literature Review," J. Biomech. Eng.

[32] Seth, A., Hicks, J. L., Uchida, T. K., Habib, A., Dembia, C. L., Dunne, J. J., Ong, C. F., DeMers, M. S., Rajagopal, A., Millard, M., Hamner, S. R., Arnold, E. M., Yong, J. R., Lakshmikanth, S. K., Sherman, M. A., Ku, J. P., and Delp, S. L., 2018, "OpenSim: Simulating Musculoskeletal Dynamics and Neuromuscular Control to Study Human and Animal Movement," PLoS Comput. Biol.

[33] Kim, Y., Jung, Y., Choi, W., Lee, K., and Koo, S., 2018, "Similarities and Differences between Musculoskeletal Simulations of OpenSim and AnyBody Modeling System," J. Mech. Sci. Technol., **32**(12), pp. 6037–6044.

[34] Karimi, M. T., Gutierrez-Farewik, L., and McGarry, A., 2019, "Evaluation of the Hip Joint Contact Force in Subjects with Perthes Based on OpenSIM," Med. Eng. Phys., **67**, pp. 44–48.

[35] Chander, H., Garner, J. C., and Wade, C., 2015, "Heel Contact Dynamics in Alternative Footwear during Slip Events," Int. J. Ind. Ergon., **48**(2015), pp. 158–166.

[36] Luczak, T., Saucier, D., Burch, R. F. V., Ball, J. E., Chander, H., Knight, A., Wei, P., and Iftekhar, T., 2018, "Closing the Wearable Gap: Mobile Systems for Kinematic Signal Monitoring of the Foot and Ankle," Electron., **7**(7), pp. 1–24.

[37] Marchetti, P. H., Jarbas da Silva, J., Jon Schoenfeld, B., Nardi, P. S. M., Pecoraro, S. L., D'Andréa Greve, J. M., and Hartigan, E., 2016, "Muscle Activation Differs between Three Different Knee Joint-Angle Positions during a Maximal Isometric Back Squat Exercise," J. Sports Med., **2016**, pp. 1–6.

[38] Stöckel, T., Jacksteit, R., Behrens, M., Skripitz, R., Bader, R., and Mau-Moeller, A., 2015, "The Mental Representation of the Human Gait in Young and Older Adults," Front. Psychol., **6**.

[39] 2017, "Gait 2392 and 2354 Models - OpenSim Documentation - Site Global" [Online]. Available: https://simtk-confluence.stanford.edu/display/OpenSim/Gait+2392+and+2354+Models. [Accessed: 11-Oct-2020].

[40] Collins, T. D., Ghoussayni, S. N., Ewins, D. J., and Kent, J. A., 2009, "A Six Degrees-of-Freedom Marker Set for Gait Analysis: Repeatability and Comparison with a Modified Helen Hayes Set," Gait Posture, **30**(2), pp. 173–180.

[41] Baker, R., Leboeuf, F., Reay, J., and Sangeux, M., 2018, "The Conventional Gait Model - Success and Limitations," *Handbook of Human Motion*, Springer International Publishing, pp. 489–508.

[42] Gray, H., 1918, *Anatomy of the Human Body - 20th Edition*, Lea and Febiger, Philadelphia.

[43] "Getting Started with Inverse Dynamics - OpenSim Documentation - Site Global" [Online]. Available: https://simtk-confluence.stanford.edu:8443/display/OpenSim/Getting+Started+with+Inverse+Dynamics. [Accessed: 14-Oct-2020].

[44] "Getting Started with RRA - OpenSim Documentation - Site Global" [Online]. Available: https://simtk-confluence.stanford.edu:8443/display/OpenSim/Getting+Started+with+RRA. [Accessed: 14-Oct-2020].

[45] "How CMC Works - OpenSim Documentation - Site Global" [Online]. Available: https://simtk-confluence.stanford.edu:8443/display/OpenSim/How+CMC+Works. [Accessed: 14-Oct-2020].

[46] Thelen, D. G., and Anderson, F. C., 2006, "Using Computed Muscle Control to Generate Forward Dynamic Simulations of Human Walking from Experimental Data," J. Biomech., **39**(6), pp. 1107–1115.

[47] Cham, R., and Redfern, M. S., 2001, "Lower Extremity Corrective Reactions to Slip Events," J. Biomech., **34**(11), pp. 1439–1445.

[48] Shroyer, J. F., and Weimar, W. H., 2010, "Comparative Analysis of Human Gait While Wearing Thong-Style Flip-Flops versus Sneakers," J. Am. Podiatr. Med. Assoc., **100**(4), pp. 251–257.

[49] Heintz, S., and Gutierrez-Farewik, E. M., 2007, "Static Optimization of Muscle Forces during Gait in Comparison to EMG-to-Force Processing Approach," Gait Posture, **26**(2), pp. 279–288.

[50] Cohen, H. H., and Cohen, D. M., 1994, "Perceptions of Walking Surface Slipperiness under Realistic Conditions, Utilizing a Slipperiness Rating Scale," J. Safety Res., **25**(1), pp. 27–31.

[51] Lee, L. F., and Umberger, B. R., 2016, "Generating Optimal Control Simulations of Musculoskeletal Movement Using OpenSim and MATLAB," PeerJ, **2016**(1).

[52] Delp, S. L., Loan, J. P., Hoy, M. G., Zajac, F. E., Topp, E. L., and Rosen, J. M., 1990, "An Interactive Graphics-Based Model of the Lower Extremity to Study Orthopaedic Surgical Procedures," IEEE Trans. Biomed. Eng., **37**(8), pp. 757–767.

APPENDIX A

EQUATIONS USED IN VARIOUS OPENSIM TOOLS

A.1 Weighted Squared Error

$$Squared\ Error = \sum_{i=1}^{markers} \omega_i (x_i^{subject} - x_i^{model})^2 + \sum_{j=1}^{joint\ angles} \omega_j (\theta_j^{subject} - \theta_j^{model})^2 \quad (6.1)$$

Where $x^{subject}$ and x^{model} are the three-dimensional positions of the ith marker or joint center for the subject and model, $\theta^{subject}$ and θ^{model} are the values of the jth joint angle for the subject and model, ω_i and ω_j are factors that allow markers and joint angles to be weighted differently [24].

A.2 Modified Newton's Second Law

$$F_{external} = \sum_{i=1}^{segments} m_i a_i - F_{residual} \quad (6.2)$$

Where $F_{external}$ is the measured ground reaction force minus the body weight vector, a_i is the translational acceleration of the center of mass of the ith body segment, m_i is the mass of the ith body segment, and $F_{residual}$ is the residual force [24].

A.3 Activation Dynamics Model

$$\dot{a} = \begin{cases} (u-a) \cdot \left[\frac{u}{\tau_{act}} + \frac{u+1}{\tau_{deact}}\right] & u > a \\ \frac{u-a}{\tau_{deact}} & u < a \end{cases} \quad (6.3)$$

Where $\dot{a}$ is the time rate of change of the muscle activation, u is the excitation and a is the muscle activation, τ_{act} and τ_{deact} are the time constants for muscle activation and deactivation [24].